THE JOURNAL OF BIOLOGICAL CHEMISTRY VOL. 285, NO. 44, pp. 33826–33833, October 29, 2010

Recombinant Membrane-targeted Form of CD59 Inhibits the Growth of Choroidal Neovascular Complex in Mice*

Received for publication, June 9, 2010, and in revised form, August 9, 2010 Published, JBC Papers in Press, August 24, 2010, DOI 10.1074/jbc.M110.153130

Nalini S. Bora[‡1], Purushottam Jha[‡], Valeriy V. Lyzogubov[‡], Sankaranarayanan Kaliappan[‡], Juan Liu[‡], Ruslana G. Tytarenko[‡], Deborah A. Fraser[§], B. Paul Morgan[§], and Puran S. Bora[‡2]

From the [‡]Department of Ophthalmology, Jones Eye Institute, Pat and Willard Walker Eye Research Center, University of Arkansas for Medical Sciences, Little Rock, Arkansas 72205 and the [§]Department of Infection, Immunity, and Biochemistry, School of Medicine, Cardiff University, Cardiff CF14 4XN, United Kingdom

This study was designed to explore the effect of recombinant, membrane-targeted CD59 (rCD59-APT542) on the growth and size of fully developed neovascular complex using the murine model of laser-induced choroidal neovascularization (CNV). CNV was induced by laser photocoagulation in C57BL/6 mice using an argon laser, and the animals received rCD59-APT542 via intravitreal (ivt) route. Western blot analysis, immunohistochemistry, and total complement hemolytic assay demonstrated that exogenously administered rCD59-APT542 was incorporated as well as retained in RPE and choroid and was functionally active *in vivo*. Single ivt injection during the growth of the CNV (*i.e.* at day 3 post-laser) resulted in ~79% inhibition of the further growth of neovascular complex. The size of the CNV complex was significantly ($p < 0.05$) reduced by the administration of rCD59-APT542 after the CNV complex has fully developed (*i.e.* at day 7 post-laser). Treatment with rCD59-APT542 blocked the formation of membrane attack complex (MAC), increased apoptosis and decreased cell proliferation in the neovascular complex. On the basis of results presented here we conclude that recombinant membrane targeted CD59 inhibited the growth of the CNV complex and reduced the size of fully developed CNV in the laser-induced mouse model. We propose that a combination of two mechanisms: increased apoptosis and decreased cell proliferation, both resulting from local inhibition of MAC, may be responsible for inhibition of CNV by rCD59-APT542.

Age-related macular degeneration (AMD)[3] is the major cause of legal blindness worldwide among the elderly (1). In AMD there is a progressive destruction of the macula leading to the loss of central vision. AMD, a complex disease with multiple risk factors (2), is usually classified into two forms, namely "dry" and "wet" type (3). Choroidal neovascularization (CNV) is the defining characteristic of wet AMD, and is responsible for the sudden and disabling loss of central vision. Laser-induced mouse model of CNV in which Bruch's membrane (BM) is disrupted by laser photocoagulation is well established and is used by an increasing number of investigators (4–7). Over the last ten years, we have noted that rodent model of laser-induced CNV has provided valuable information and contributed significantly to our understanding of the underlying mechanisms involved in the pathogenesis of new vessel growth from the choroid (7–10).

Evidence from both human and animal studies supports a key role for complement activation in the development of CNV (7–11). We demonstrated that membrane attack complex (MAC) formation via the alternative pathway activation is important for the release of angiogenic growth factors that are critical for the induction of CNV in mouse model (9). Using the mouse model of laser-induced CNV we further reported that recombinant soluble (rs) CD59a-Fc controls the induction of CNV (10). CD59 is a complement regulatory protein (CReg) that controls the formation and function of MAC. In mouse, the CD59 gene is duplicated, and two genes termed CD59a and CD59b show differential tissue distribution (12, 13). CD59a is the primary regulator of MAC in mice (12). Interestingly, administration of rsCD59a-Fc inhibited the development of the CNV complex in the mouse model by blocking MAC formation and inhibiting the expression of angiogenic growth factors (10). Our initial results demonstrated that the growth of the CNV complex or the size of fully developed neovascular complex was not affected by treatment with rsCD59a-Fc. This may be due to the fact that although rsCD59a-Fc is an efficient complement inhibitor, its bioavailability and limited local retention at the site of interest limit its capacity to efficiently inhibit MAC formation as a result of increased complement activation during the growth of CNV. One way of improving local protein retention is by adding a membrane-targeting moiety (14–16). CD59 containing a membrane targeting moiety (APT542) has been reported to bind firmly to the cell surface and is 100-fold more effective in inhibiting complement activation and MAC deposition than the untargeted protein (15). The purpose of the present study was to investigate if the growth of the CNV complex as well as the size of fully developed CNV can be inhibited

* This work was supported in, whole or in part, by National Institutes of Health Grants EY014623 and EY018812, and the Pat & Willard Walker Eye Research Center, Jones Eye Institute, University of Arkansas for Medical Sciences, Little Rock, AR.

[1] To whom correspondence may be addressed: Dept. of Ophthalmology, Jones Eye Institute, University of Arkansas for Medical Sciences, 4301 West Markham, 523 Little Rock, AR 72205-7199. Tel.: 501-686-8293; Fax: 501-686-8316; E-mail: NBora@UAMS.edu.

[2] To whom correspondence may be addressed: Dept. of Ophthalmology, Jones Eye Institute, University of Arkansas for Medical Sciences, 4301 West Markham, 523 Little Rock, AR 72205-7199. Tel.: 501-686-8293; Fax: 501-686-8316; E-mail: PBora@UAMS.edu.

[3] The abbreviations used are: AMD, age-related macular degeneration; CNV, choroidal neovascularization; RPE, retinal pigment epithelium; MAC, membrane attack complex; rsCD59a-Fc, recombinant soluble CD59a-Fc; rCD59-APT542, recombinant membrane-targeted CD59; ivt, intravitreal; NHS, normal human serum; PCNA, proliferating cell nuclear antigen; TUNEL, terminal deoxynucleotidyltransferase-mediated dUTP nick end-labeling.

by recombinant membrane targeted CD59 (rCD59-APT542) and compare its *in vivo* effectiveness to rsCD59a-Fc. Recombinant membrane targeted CD59 (rCD59-APT542) was prepared as previously described by coupling the soluble rat CD59 through its C terminus to a short, synthetic address tag termed APT542 (15). This protein inhibits the complement system of both rat and mouse (15). In the current study we also explored the underlying mechanisms of rCD59-APT542 mediated inhibition of CNV.

EXPERIMENTAL PROCEDURES

Animals—Male C57BL/6 mice (6–8 weeks old) were purchased from the Jackson Laboratory (Bar Harbor, ME). This study was approved by the Institutional Animal Care and Use Committee (IACUC), University of Arkansas for Medical Sciences, Little Rock, AR.

Administration of Recombinant CD59 (rCD59-APT542) in Naïve Mice—Recombinant membrane targeted CD59 (rCD59-APT542) was prepared as previously described (15). Naïve C57BL/6 mice were divided into two groups. Animals in group 1 received a single intravitreal (ivt) injection (25 μg in 2 μl) of rat rCD59-APT542 while the animals in group 2 received a similar treatment with sterile PBS. Animals in both the groups were sacrificed at day 5 (n = 3 mice) post-injection and RPE-choroid harvested from these animals were pooled separately. The tissue was homogenized, solubilized in PBS, and the protein samples were used in the "Complement Hemolytic Assay" and Western blot analysis described below. Because protease inhibitors and Nonidet P-40 interfere with "Complement Hemolytic Assay", they were not added to the PBS used to soublize RPE and choroid used in "Complement Hemolytic Assay." For Western blot analysis RPE-choroid tissue was homogenized in PBS containing 1% protease inhibitors and 1% Nonidet P-40. The experiment was repeated three times.

Complement Hemolytic Assay—Protein samples (25 μl) extracted from RPE-choroid harvested from CD59-APT542 or PBS injected mice were incubated *in vitro* with 50 μl of normal human serum (NHS) at 37 °C for 30 min as previously described (17). Different dilutions of this mixture were assayed for the inhibition of complement-dependent serum hemolytic activity as described before (7, 17) using sensitized sheep erythrocytes (Diamedix, Miami, FL). Normal human serum (NHS) not treated with protein samples but treated *in vitro* with the same volume of PBS was used as the positive control, and serum hemolytic activity of this sample was taken as 100%.

Western Blot Analysis—After SDS-PAGE on 12% linear slab gel, separated proteins were transferred to a polyvinylidene fluoride membrane. Blots were blocked in 5% BSA for 1 h at room temperature. Blots were incubated with rabbit polyclonal antibody raised against amino acids 1–123 representing full-length CD59a of mouse origin (1:500; FL-123, Santa Cruz Biotechnology) or monoclonal anti-β actin (1:10,000; mouse IgG1; Sigma-Aldrich) overnight at 4 °C. Control blots were treated with the same dilution of appropriate IgG isotype control. After washing and incubation with HRP-conjugated secondary Ab (1:5000 dilution; Santa Cruz Biotechnology), blots were developed using the ECL Western blot analysis detection system (ECL Plus; Amersham Biosciences).

Induction of CNV, Administration of rCD59-APT542 and rsCD59a-Fc—CNV was induced by laser photocoagulation in C57BL/6 mice with an argon laser (50-μm spot size, 0.05 s duration, 260 milliwatt) as previously described by us (7–9). Three laser spots were placed in each eye close to the optic nerve. In our initial experiments three different doses (12.5 μg in 2 μl of PBS, 25 μg in 2 μl of PBS, and 50 μg in 2 μl of PBS) of rat rCD59-APT542 were used for intravitreal injections. Intravitreal (25 μg) gave the best results and was used in subsequent experiments. CD59a coupled to mouse IgG Fc (rsCD59aFc) was prepared as previously described (13). In these experiments 75 μg of rsCD59a-Fc in 2 μl of PBS was injected via ivt route and this dose of rsCD59a-Fc was selected on the basis of our experience with this protein. Animals were divided into six groups (n = 5 mice/group). Animals received a single ivt injection of rCD59-APT542 (group 1) or rsCD59a-Fc (group 2) on day 3 post-laser. Control animals (group 3) received similar treatments with sterile PBS. Animals in group 1, 2, and 3 were sacrificed at day 7 post-laser treatment. In another set of experiments C57BL/6 mice received a single ivt injection of rCD59-APT542 (group 4) or rsCD59a-Fc (group 5) on day 7 after laser. Mice in group 6 received a single ivt injection of PBS at day 7 post-laser. Animals in group 4, 5, and 6 were sacrificed at day 9 post-laser. Experiments were repeated three times.

Measurement of Neovascular Complex—Mice were anesthetized (ketamine/xylazine) and perfused through the heart with 1 ml PBS containing 50 mg/ml fluorescein labeled dextran (FITC-dextran, 2 million average molecular weight, Sigma). The eyes were removed and fixed for 1 h in 10% phosphate-buffered formalin. The cornea and the lens were removed and the neurosensory retina was carefully dissected from the eyecup. Five radial cuts were made from the edge of the eyecup to the equator and RPE-choroid-sclera tissue was stained with a mAb against elastin (Sigma) and a Cy3-conjugated secondary antibody (Sigma).

RPE-choroid-sclera tissue was flat-mounted, with the sclera facing down, on a glass slide in Aqua mount. Flat mounts were examined under a confocal microscope (Zeiss LSM510). The CNV stained green whereas the elastin stained red. The percentage of FITC-dextran perfused vessels in laser injured zones was measured with ImagePro Plus software (Media Cybernetics, Inc. Bethesda, MD).

MAC ELISA—In preliminary experiments, the capacity of a human SC5b-9 EIA kit (Quidel Corp.) to detect mouse SC5b-9/MAC was tested by comparing values obtained with normal human serum (unactivated or zymosan activated) and normal mouse serum (unactivated or zymosan activated). RPE-choroid tissue harvested from six mice was homogenized in 500 μl of lysis buffer (PBS with 1% of Nonidet P-40 and 1% of protease inhibitor) on ice. The lysate was centrifuged at 10,000 rpm for 10 min at 4 °C, and MAC levels in the supernatant were detected using human SC5b-9 Plus EIA kit and normalized to total protein concentration. ELISA was performed according to the manufacturer's recommendations. The concentration of MAC was calculated by computer software using the standard curves obtained from known concentrations (EIA kit).

Immunohistochemistry—Mice injected ivt with CD59-APT542 or PBS at day 3 post-laser (n = 5 mice/group) were

sacrificed at day 7 post-laser. Another set of mice ($n = 5$ mice/group) received a single ivt injection of CD59-APT542 at day 7 and were sacrificed at day 9 post-laser. Eyes were harvested, fixed in 10% formalin solution (Sigma-Aldrich) and embedded in paraffin. The paraffin-embedded tissue sections (4 μm) were immunostained for terminal deoxynucleotidyl transferase (TdT)-mediated d-UTP-FITC nick end labeling (TUNEL), MAC and proliferating-cell nuclear antigen (PCNA). TUNEL staining was performed using the kit purchased from Roche (Indianapolis, IN) according to the manufacturer's instructions. For MAC detection, polyclonal rabbit anti-rat/mouse C9 (1:1000) was used as the primary antibody. PCNA was detected using goat polyclonal anti-PCNA antibody (1:500; Biovision, Mountain View, CA). AlexaFluor 594 conjugated goat anti-rabbit IgG (Invitrogen) was used as the secondary antibody for MAC staining. AlexaFluor 594 conjugated donkey anti-goat IgG (Invitrogen) was used as the secondary antibody for detecting PCNA. Mouse monoclonal anti-rat CD59 (6D1, mouse IgG1; 1:100) and M.O.M. Immunodetection kit (Vector Laboratories, Burlingame, CA) were used to localize rat CD59-APT542 in mouse RPE and choroid. Control stains were performed with non-relevant antibodies of the same Ig subclass at concentrations similar to those of the primary antibodies. Additional controls consisted of staining by omission of the primary or secondary antibody. After staining with the secondary antibody, the sections were covered with mounting medium (ProLong Gold Mounting Medium; Invitrogen). The slides were examined under a ZEISS LSM 510 confocal microscope. TUNEL- and PCNA-stained sections from each laser injured area were captured and a total of 30 laser spots sections per group were investigated. TUNEL- and PCNA-positive cells in laser injured area were counted in a masked fashion. For MAC staining images of red fluorescence in each laser-injured area were captured with Q Imaging GO-5 digital camera and confocal microscope. The intensity of red fluorescence was analyzed using ImageJ 1.40g (NIH), and the intensity was measured as integrated density using the software.

Statistical Analysis—The data are expressed as the mean ± S.D. Data were analyzed and compared using Student's t test, and differences were considered statistically significant with $p < 0.05$.

RESULTS

Incorporation and/or Retention of Exogenously Administered rCD59-APT542 in RPE and Choroid of Naïve Mice—To establish that exogenously administered membrane targeted form of recombinant rat CD59 (rCD59-APT542) was incorporated in RPE and choroid; naïve C57BL/6 mice received a single ivt injection of rCD59-APT-542. Animals were sacrificed on day 5 post-injection ($n = 3$ mice) and RPE and choroid tissue was used in Western blot analysis. Rabbit polyclonal anti-CD59 (FL-123) was used in Western blot analysis to distinguish endogenous murine CD59 from exogenously administered recombinant rat CD59 (rCD59-APT542). Western blot analysis demonstrated the presence of constitutively expressed murine CD59a (~19 kDa) in RPE-choroid harvested from both PBS and rCD59-APT-542 treated animals (Fig. 1*A*, *lanes 1* and *2*). Exogenously administered rat rCD59-APT542 (~11 kDa) was

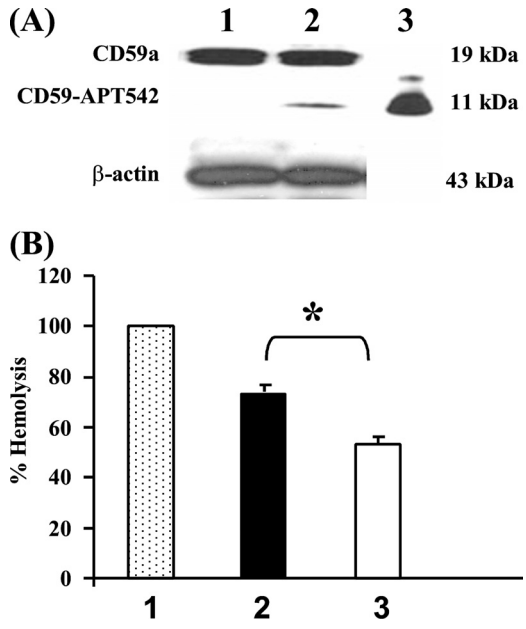

FIGURE 1. **Retention and complement-inhibitory activity of rCD59-APT542 in RPE and choroid of naïve mouse eye.** Naïve C57BL/6 mice injected separately via the ivt route with rat rCD59-APT542 or PBS were sacrificed at day 5 post-injection, and total protein was extracted from harvested RPE and choroid. *A*, representative Western blot of RPE-choroid protein samples from mice treated ivt with PBS (*lane 1*) or injected ivt with rCD59-APT542 (*lane 2*) using polyclonal antibody reactive with mouse/rat CD59. A strong band of 19 kDa in *lanes 1* and *2* represents murine CD59 constitutively expressed by the resident RPE and choroidal cells. Note that the 11 kDa protein band representing exogenously administered rat rCD59-APT542 was detected only in rCD59-APT542-injected mice (*lane 2*) and not in mice treated similarly with PBS alone (*lane 1*). Purified CD59-APT542 was loaded in *lane 3* and served as the positive control. *Panel B* demonstrates the complement inhibitory activity of protein samples prepared from RPE-choroid of mice injected ivt with PBS (■, 2) or rat CD59-APT542 (□, 3) in complement hemolytic assay using normal human serum (NHS). Animals were sacrificed on day 5 postinjection. NHS (▨, 1) not treated with protein samples but treated *in vitro* with the same volume of PBS was used as the positive control and serum hemolytic activity of this sample was taken as 100%. Data are represented as mean ± S.D. of triplicate determinations. *, $p < 0.05$.

detected in RPE-choroid harvested from mice injected with rCD59-APT542 on day 5 (Fig. 1*A*, *lane 2*) post-injection. In contrast, the 11 kDa band representing rat rCD59-APT542 was not present in the RPE-choroid from the PBS injected mice (Fig. 1*A*, *lane 1*). A strong band of equal intensity at 43 kDa for β-actin in *lanes 1* and *2* indicated equal amount of total protein in both lanes (Fig. 1*A*). Purified rat rCD59-APT542 was used as the positive control and was loaded in *lane 3* (Fig. 1*A*).

Exogenously Administered rCD59-APT542 Is Functionally Active—Complement hemolytic assay was utilized to determine that rCD59-APT542 incorporated in RPE and choroid is functionally active. Naïve C57BL/6 mice received a single ivt injection of rCD59-APT542 or PBS and were sacrificed on day 5 post-injection ($n = 3$ mice). RPE and choroid were harvested and normal human serum (NHS) was treated separately with protein extracted from RPE-choroid harvested from these mice. NHS not treated with protein samples but treated *in vitro* with the same volume of PBS was used as the positive control and serum hemolytic activity of this sample was taken as 100% (Fig. 1*B*). As shown in Fig. 1*B*, protein samples prepared from RPE-choroid inhibited the complement-mediated lysis of sensitized SRBCs by NHS. Treatment of NHS with protein sample

prepared from RPE-choroid of PBS injected mice resulted in ~25% inhibition of the total hemolytic activity of NHS. This complement inhibitory activity is due both to nonspecific protein effects and to various complement regulatory proteins expressed constitutively on the RPE and choroid of PBS injected mice. Similar treatment of NHS with the RPE-choroid protein samples harvested from rCD59-APT542 injected mice decreased the total hemolytic activity of NHS by ~ 45% (Fig. 1*B*). This additional (25–27%) inhibition of hemolytic activity by protein samples from rCD59-APT542 treated mice represents the complement inhibitory activity of exogenously administered rCD59-APT542 protein. Exogenously administered rCD59-APT542 contributes to the increased inhibition of total hemolytic complement activity observed in protein samples prepared from the eyes of rCD59-APT542-injected mice. Collectively, our results demonstrated that ivt-injected rat rCD59-APT542 reached the RPE and choroid, was locally retained and functionally active.

Effect of rCD59-APT542 and rsCD59a-Fc Administration on the CNV Complex—Based on our previous studies and reports from other investigators (4, 7, 9, 10, 18–21), laser-induced CNV in mice can be arbitrarily divided into three phases, the induction phase (days 1–2 post-laser), the growth phase (days 3–6 post-laser), and the mature phase (days 7–14 post-laser). In the current study, rCD59-APT542 and rsCD59a-Fc were injected separately on day 3 or day 7 post-laser to investigate the effect of these agents on the growth of the CNV complex and on the size of the fully developed CNV complex, respectively.

Effect of rCD59-APT542 and rsCD59a-Fc Administration on the Growth of the CNV Complex—We studied the effect of local (ivt) injection of rCD59-APT542 and rsCD59a-Fc on the growth of the CNV complex using mouse model of laser-induced CNV. A single dose of rCD59-APT542 (25 μg) or rsCD59a-Fc (75 μg) was delivered via ivt route during the growth of the CNV complex (*i.e.* at day 3 post-laser), and the animals were sacrificed at day 7 after laser treatment. Control animals received a similar treatment with sterile PBS. Confocal analysis of RPE-choroid-sclera flat mounts demonstrated that the further growth of neovascular complex was significantly (~79%, $p < 0.05$) inhibited by a single ivt injection of rCD59-APT542 in all C57BL/6 mice (Fig. 2, *B* and *D*). Similar administration of 75 μg of rsCD59a-Fc (Fig. 2, *C* and *D*) or sterile PBS (Fig. 2, *A* and *D*) did not affect the growth of the CNV complex.

Effect of rCD59-APT542 and rsCD59a-Fc on the Size of the Fully Developed CNV Complex—We next investigated if the administration of rCD59-APT542 or rsCD59a-Fc in the animals with fully developed CNV affects the size of neovascular complex. In this model, the CNV complex fully develops by day 7 post-laser (7–10). C57BL/6 mice received a single ivt injection (25 μg) of rCD59-APT542 or rsCD59a-Fc (75 μg) at day 7 and were sacrificed at day 9 after laser treatment. Our results demonstrate that treatment with rCD59-APT542 resulted in significantly ($p < 0.05$) decreased (~44%) size of the CNV complex (Fig. 3, *B* and *D*) in all mice compared with rsCD59a-Fc (Fig. 3, *C* and *D*) and PBS-injected animals (Fig. 3, *A* and *D*).

Taken together our above mentioned results demonstrated that administration of rCD59-APT542 during the growth phase of laser-induced CNV or after the CNV complex is fully developed inhibited neovascular complex in C57BL/6 mice. In contrast, the growth of the CNV complex or the size of fully developed neovascular complex was not affected by treatment with rsCD59a-Fc.

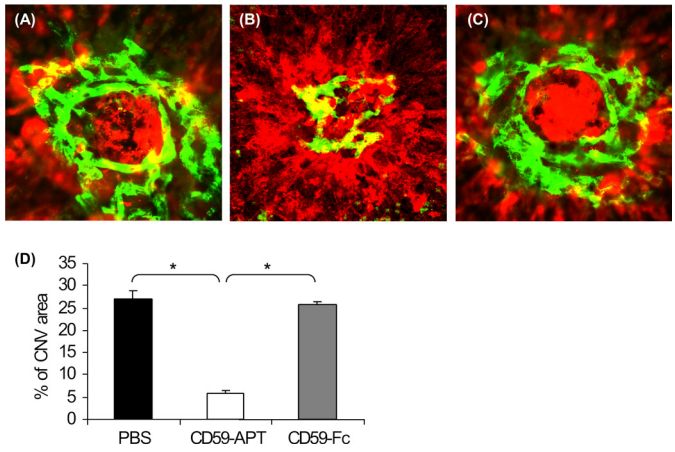

FIGURE 2. **Effect of rCD59-APT542 administration on the growth of neovascular complex.** C57BL/6 mice were injected intravitreally with PBS (*A*) or rat rCD59-APT542 (*B*) or rsCD59a-Fc (*C*) at day 3 post-lasers and were sacrificed at day 7 after laser treatment. Representative confocal micrograph of the neovascular complex shows new vessels as *green* and *red* color for elastin. The growth of the CNV complex was significantly reduced in rCD59-APT542 (□) injected C57BL/6 mice compared with PBS (■)- and rsCD59a-Fc (▩)-injected animals (*D*). *, $p < 0.05$.

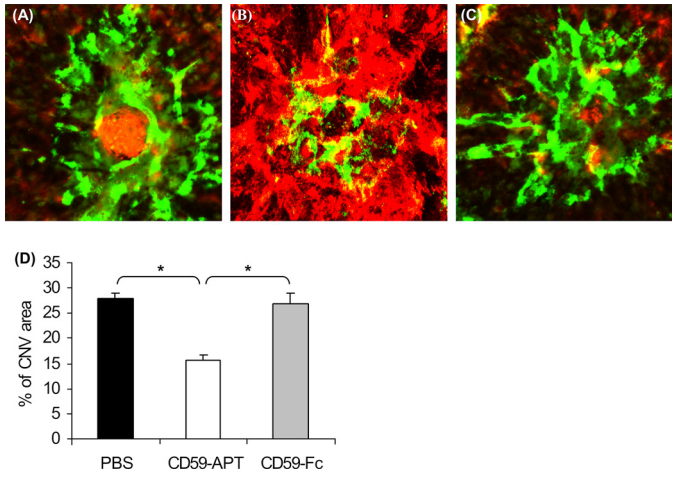

FIGURE 3. **Effect of rCD59-APT542 administration on the size of fully developed neovascular complex.** Representative confocal micrograph of RPE-choroid-sclera flat mounts from mice injected with rat rCD59-APT542 ivt (*B*) on day 7 and sacrificed at day 9 after laser treatment. Another set of animals were treated similarly with PBS (*A*) or rsCD59a-Fc (*C*). The size of the CNV complex was significantly reduced in rCD59-APT542 (□)-injected C57BL/6 mice compared with PBS (■)- and rsCD59a-Fc (▩)-injected animals (*D*). *, $p < 0.05$.

Localization of rCD59-APT542 in RPE and Choroid of Laser-treated Mice—rCD59-APT542 and PBS were injected separately in C57BL/6 mice via ivt route at day 7 post-laser. Animals were sacrificed at day 9 after laser treatment and localization of rat rCD59-APT542 was performed by immunohistochemistry using monoclonal anti-rat CD59 antibody (6D1). This antibody recognizes rat CD59 only and does not cross-react with endogenous murine CD59. In mice injected with rCD59-APT542, RPE and choroid stained strongly for exogenously administered rat protein in the area of no laser injury (Fig. 4*A*) as well as in the laser-injured area (Fig. 4*B*). However, no staining for rCD59-

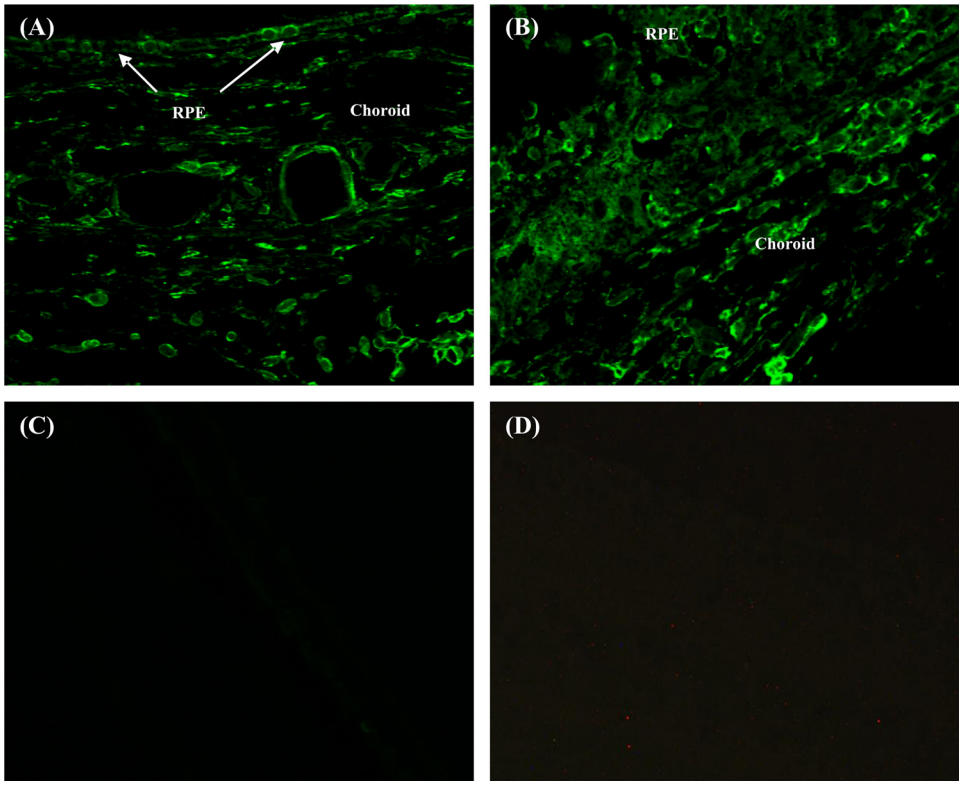

FIGURE 4. **Localization of rCD59-APT542 in the eye of laser-treated mice.** C57BL/6 mice received rat CD59-APT542 or PBS at day 7 post-laser. Animals were sacrificed at day 9 after laser treatment, and eyes were processed for paraffin sectioning. Sections were stained with mouse monoclonal anti-rat CD59 (6D1). This antibody (6D1) recognizes rat CD59 only and does not cross-react with endogenous murine CD59. Strong staining for exogenously administered CD59-APT542 was detected on RPE and choroid in the area of no-laser injury (*A*) as well in the laser-injured area (*B*) of CD59-APT542 injected mice. No staining for CD59-APT542 was detected in PBS-injected mice (*C*). No staining was observed in the control sections stained without the primary antibody (*D*). Objective magnification: ×63.

APT542 was detected in PBS-injected mice (Fig. 4*C*). Control sections stained without the primary antibody showed no staining (Fig. 4*D*). Similar results were obtained in animals injected ivt with rat rCD59-APT542 at day 3 and sacrificed at day 7 post-laser treatment (data not shown). Collectively, our results demonstrated that intravitreally administered rCD59-APT542 localized to RPE and choroid of laser-treated C57BL/6 mice.

Mechanism of rCD59-APT542-mediated Inhibition of CNV Growth—We also explored the underlying mechanism responsible for above mentioned effects of rCD59-APT542 during the growth of CNV as well as on the fully developed CNV complex. We investigated the apoptosis of cells in the neovascular complex by TUNEL assay whereas the proliferation of cells in the neovascular complex was examined by staining for cell proliferation marker, PCNA. MAC deposition was determined using immunohistochemistry or a human SC5b-9 EIA kit. Capacity of human SC5b-9 EIA kit to detect mouse SC5b-9 was proven by showing that, while normal mouse serum gave no signal in the assay, after zymosan activation mouse serum was strongly positive in the assay (values ~12-fold lower than in zymosan-activated human serum).

Growth Phase—Laser-treated C57BL/6 mice were divided into two groups ($n = 5$ mice/group). Mice in group 1 received a single intravitreal injection of rCD59-APT542 on day 3 post-laser and mice in group 2 (control) received a similar treatment with PBS. Animals in both groups 1 and 2 were sacrificed on day 7 post-laser. $TUNEL^+$ fluorescent cells were barely detectable in laser-injured area of PBS-treated mice (Fig. 5*B*). In contrast, several $TUNEL^+$ fluorescent cells were detected in the laser-injured area of rCD59-APT542-injected mice (Fig. 5*A*). These differences were statistically ($p < 0.05$) significant (Fig. 5*C*). The effect of rCD59-APT542 treatment on the proliferation of cells in the CNV complex was investigated by immunofluorescent staining of paraffin sections for the cell proliferation marker, PCNA. Fewer cells stained for PCNA in the laser spot of the mice that were injected with rCD59-APT542 (Fig. 5*D*) compared with PBS-treated control mice (Fig. 5*E*), and these differences were statistically ($p < 0.05$) significant (Fig. 5*F*). Our results revealed significantly (Fig. 5*I*; $p < 0.05$) reduced MAC deposition at day 7 post-laser in the laser-injured area of the mice that received rCD59-APT542 injection at day 3 post-laser (Fig. 5, *G* and *I*) compared with PBS-treated control mice (Fig. 5, *H* and *I*).

Maturation Phase—Animals were divided into two groups ($n = 5$ mice/group). Animals in group 1 received single intravitreal injection of rCD59-APT542 on day 7 post-laser and sacrificed on day 9 post-laser. Mice in group 2 received PBS on day 7 and were sacrificed on day 9. Few $TUNEL^+$ fluorescent cells were detected in the laser spots of PBS-treated mice sacrificed on day 9 (Fig. 6*B*). However, the administration of rCD59-APT542 at day 7 resulted in a significant (Fig. 6*C*; $p < 0.05$) increase in the number of $TUNEL^+$ fluorescent cells in the laser spots at day 9 (Fig. 6, *A* and *C*). Next we investigated the effect of rCD59-APT542 treatment on cell proliferation in laser injured area. As shown in Fig. 6, few cells stained for PCNA in the laser-injured area, and no statistically significant (Fig. 6*F*; $p > 0.05$) difference in the number of PCNA-positive cells was observed between rCD59-APT542 (Fig. 6, *D* and *F*)-treated mice and PBS-treated mice (Fig. 6, *E* and *F*) on day 9 post-laser. At day 9, post-laser levels of MAC were almost undetectable in both rCD59-APT542- and PBS-treated mice using immunohistochemistry (Fig. 7, *A* and *B*). Because we were unable to detect any difference in MAC levels visually between PBS- and rCD59-APT542-injected mice at day 9 post-laser using immunohistochemistry, we used ELISA to see if we can detect any difference in the levels of MAC between the two groups at this time point. Our results presented in Fig. 7*C* demonstrated that administration of rCD59-APT542 resulted in significantly ($p < 0.05$) lower levels of MAC in RPE and choroid of rCD59-APT542-treated mice compared with PBS-treated mice on day 9 post-laser.

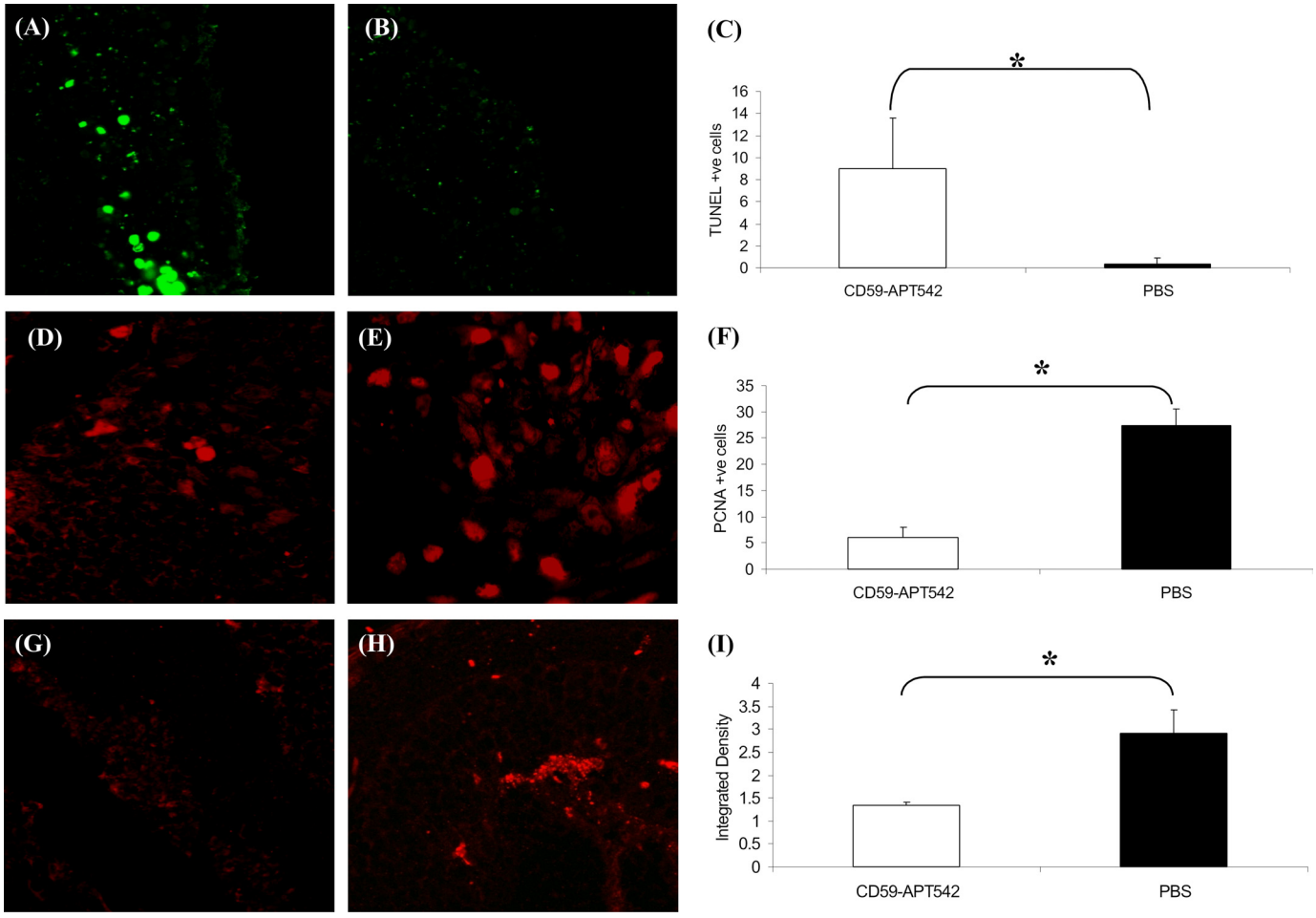

FIGURE 5. **Effect of rCD59-APT542 on apoptosis, cell proliferation, and MAC during the growth of laser-induced CNV.** Representative confocal micrograph of paraffin sections of laser-injured area stained for TUNEL (*A* and *B*), PCNA (*D* and *E*), and MAC (*G* and *H*). Mice were lasered (day 0) and injected ivt with rat CD59-APT542 or PBS at day 3 post-laser. Animals were sacrificed at day 7 post-laser, and eyes were processed for paraffin sectioning. Many TUNEL$^+$ cells (green fluorescence) were detected in laser-injured area of CD59-APT542-treated mice (*A*). In contrast TUNEL$^+$ cells were barely detected in PBS-treated mice (*B*). *C* represents cumulative data for TUNEL$^+$ cells. Antibody specific for the cell proliferation marker PCNA was used to stain the proliferating cells (*D* and *E*). Less PCNA$^+$ cells were detected in laser-injured area of CD59-APT542 injected mice (*D*) compared with PBS treated mice (*E*). *F* represents cumulative data for PCNA$^+$ cells. Low levels of MAC were detected in the laser-injured area of CD59-APT542 (*G*)-treated mice compared with PBS (*H*)-treated mice. *I* represents integrated density of MAC staining as measured by ImageJ 1.40g software. Objective magnification: ×63. *, $p < 0.05$.

Taken together, our results clearly demonstrated that intravitreal injection of rCD59-APT542 during the growth of CNV (day 3 post-laser) as well as when CNV is fully developed (day 7 post-laser) decreases MAC deposition, increases apoptosis, and decreases cell proliferation in the CNV complex.

DISCUSSION

Angiogenic neovascular changes in the choroid (CNV) are the hallmark of wet AMD and cause of sudden loss of vision in people over the age of 55. We have previously reported that administration of recombinant soluble (rs) CD59a-Fc before laser treatment inhibited the development of CNV by blocking the formation of MAC and inhibiting angiogenic growth factors (10). In the present study, we used CD59-APT542 to inhibit the growth of CNV and compared its effectiveness to rsCD59a-Fc. CD59-APT542 is a recombinant protein generated by fusing a short, synthetic address tag (APT542) to rat recombinant CD59 (15). Recombinant CD59-APT 542 has been reported to be an efficient and specific *in vivo* inhibitor of MAC activity in both rat and mouse (15).

Our results from the present investigation demonstrated that rCD59-APT542 injected via intravitreal route was able to reach RPE and choroid of the naïve mouse eye and this recombinant protein was retained locally for at least 5 days. Furthermore, rCD59-APT542 incorporated and/or retained in RPE and choroid of naïve eye was functionally active. Importantly, our results demonstrated that intravitreally administered rCD59-APT542 localized to RPE and choroid of laser treated mice as well. We have shown in this study that local administration of rCD59-APT542 during the growth phase of neovascular complex significantly inhibited the further growth of the CNV complex. In addition, rCD59-APT542 significantly reduced the size of a fully developed neovascular complex, raising the possibility that such a treatment might be effective in established disease. In contrast, there was no effect on CNV when rsCD59a-Fc was administered during the growth of the CNV complex or when the CNV complex is fully developed. It has previously been reported that a single intraarticular administration of rCD59-APT542 markedly

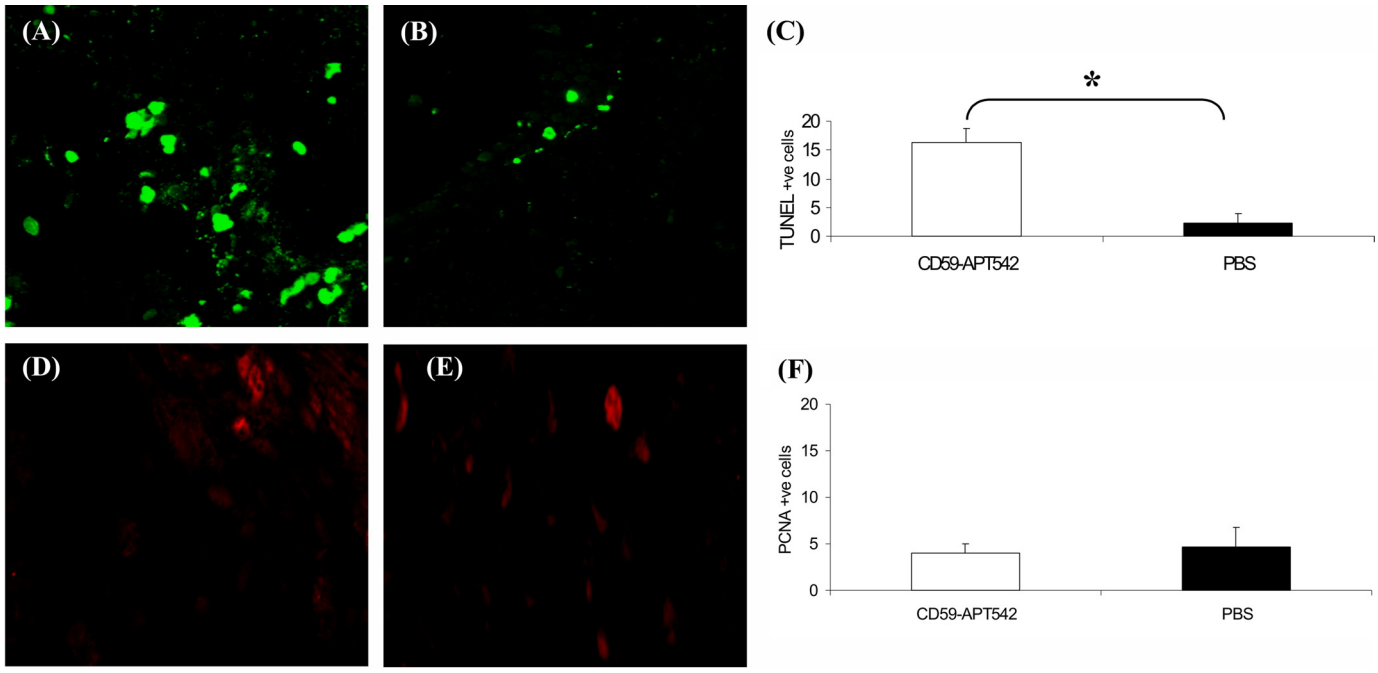

FIGURE 6. **Effect of rCD59-APT542 administration on apoptosis and cell proliferation after the CNV complex is fully developed.** Mice were lasered (day 0) and injected ivt with rat CD59-APT542 or PBS at day 7 post-laser. Animals were sacrificed at day 9 post-laser. Representative confocal micrograph of paraffin sections of laser-injured area stained for TUNEL (*A* and *B*) and PCNA (*D* and *E*). Increased number of TUNEL$^+$ cells (green fluorescence) were observed in the laser-injured area of CD59-APT542-treated mice (*A*) compared with PBS-treated mice (*B*). *C* represents cumulative data for TUNEL$^+$ cells. Few PCNA$^+$ cells were present in the laser-injured area of CD59-APT542 (*D*)- and PBS (*E*)-treated mice. *F* represents cumulative data for PCNA$^+$ cells. Objective magnification: ×63. *, $p < 0.05$.

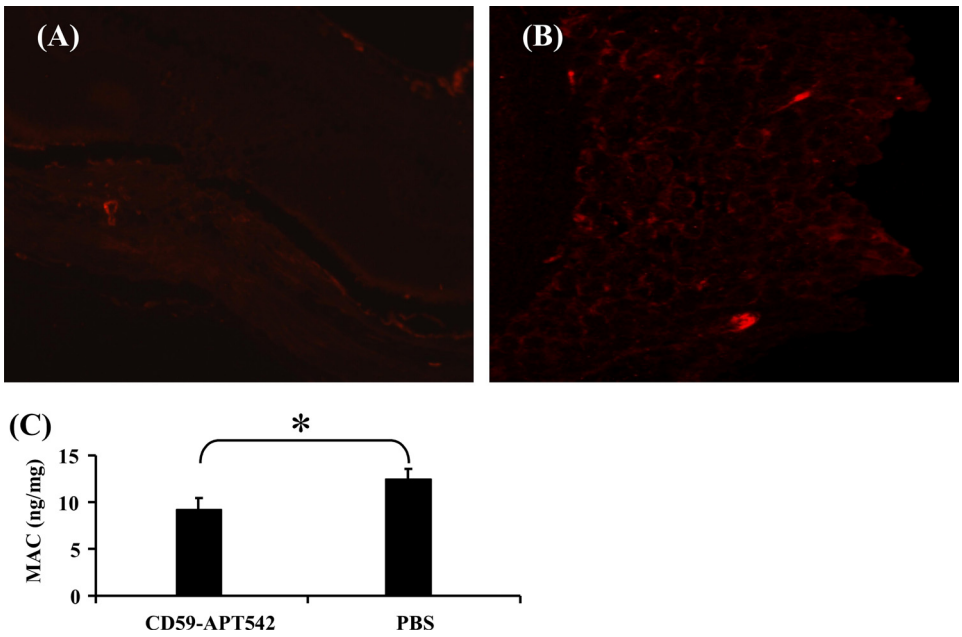

FIGURE 7. **Effect of rCD59-APT542 administration on MAC after the CNV complex is fully developed.** Mice were lasered (day 0) and injected ivt with rat CD59-APT542 or PBS at day 7 post-laser. Animals were sacrificed at day 9 post-laser. Representative confocal micrograph of paraffin sections of laser-injured area stained for MAC (*A* and *B*). Using immunohistochemical analysis MAC was almost undetectable in CD59-APT542-treated mice (*A*) and PBS-treated mice (*B*). ELISA for MAC (*C*). Low levels of MAC were detected using ELISA in RPE-choroid of PBS-treated mice at day 9 post-laser. CD59-APT542 treatment at day 7 resulted in a further decrease in MAC levels at day 9 post-laser. Objective magnification: ×63. *, $p < 0.05$.

reduced the disease severity in a murine model of rheumatoid arthritis, and was more effective than soluble rCD59 again implying retention at the site of injection (15).

The inhibitory effect of rCD59-APT542 on CNV observed in our study can be attributed to reduced levels of MAC. MAC has been implicated as a stimulus to cell proliferation in both *in vitro* and *in vivo* studies and sublytic levels of MAC have been directly implicated in stimulating cell proliferation under pathological conditions (22–26). Administration of rCD59-APT542 during the growth of the CNV complex observed in our study resulted in reduced MAC formation that leads to reduced cell proliferation. Interestingly, after CNV is fully developed we did not observe any difference in the number of proliferating cells in the CNV complex of rCD59-APT542- and PBS-treated mice by staining for PCNA. This may be due to the fact that in the mouse model of laser-induced CNV, at day 7 post-laser most of the cells in the CNV complex are mature and proliferate at a very low rate (18, 19).

In addition to the effect of MAC on cell proliferation, reduction of CNV size by rCD59-APT542 reported in the current study may involve MAC-mediated apoptosis. MAC at low levels has been reported to play a role in modulating apoptosis (22, 27–29). We observed an increase in the number of cells undergoing apoptosis in the CNV complex of mice treated with rCD59-APT542

compared with control animals during the growth of CNV. Also, the number of cells undergoing apoptosis increased while the levels of MAC decreased in mice injected with rCD59-APT542 after the CNV complex is fully developed compared with control mice.

In conclusion, we report two novel findings in this manuscript. First, recombinant membrane-targeted CD59 inhibited the growth of the CNV complex as well as the size of fully developed CNV lesions in the laser-induced mouse model. Second, our results suggest that a combination of two mechanisms: 1) decreased cell proliferation; 2) increase in the number of cells undergoing apoptosis, both resulting from low levels of MAC caused by rCD59-APT542 lead to inhibition of CNV. Additionally, this may also be in part due to decreased levels of growth factors. We have previously reported that blockade of MAC formation by complement depletion (7), inhibition of the alternative pathway (9), or by administration of rsCD59a-Fc (10) inhibited angiogenic growth factors in C57BL/6 mice with laser-induced CNV.

The inhibition of CNV during the growth and after the CNV complex is fully developed as observed in our current study is of great clinical relevance because the experiments described here mimic frequent clinical presentation in humans. On the basis of the results presented here we believe that membrane targeted recombinant CD59 may have potential to treat human AMD. Recombinant membrane targeted CD59 may be a better therapeutic agent in humans than strategies targeting C3 or C5 because CD59 inhibits the complement system at the terminal step without affecting upstream events that play crucial roles in host defense.

Acknowledgments—We thank Dr. Claire L. Harris and Dr. Richard A. Smith for helpful comments. The Digital and Confocal Microscopy Laboratory, University of Arkansas for Medical Sciences was supported by National Institutes of Health Grant 2P20 RR16460 and National Institutes of Health/NCRR Grant 1 S10 RR 19395.

REFERENCES

1. Ferris, F. L., 3rd, Fine, S. L., and Hyman, L. (1984) *Arch. Ophthalmol.* **102,** 1640–1642
2. Evans, J. R. (2001) *Prog. Retinal. Eye Res.* **20,** 227–253
3. Fine, S. L., Berger, J. W., Maguire, M. G., and Ho, A. C. (2000) *N. Engl. J. Med.* **342,** 483–492
4. Campochiaro, P. A. (2000) *J. Cell. Physiol.* **184,** 301–310
5. Ryan, S. J. (1979) *Trans. Am. Ophthalmol. Soc.* **77,** 707–745
6. Husain, D., Ambati, B., Adamis, A. P., and Miller, J. W. (2002) *Ophthalmol. Clin. North Am.* **15,** 87–91
7. Bora, P. S., Sohn, J. H., Cruz, J. M., Jha, P., Nishihori, H., Wang, Y., Kaliappan, S., Kaplan, H. J., and Bora, N. S. (2005) *J. Immunol.* **174,** 491–497
8. Bora, P. S., Kaliappan, S., Xu, Q., Kumar, S., Wang, Y., Kaplan, H. J., and Bora, N. S. (2006) *FEBS J.* **273,** 1403–1414
9. Bora, N. S., Kaliappan, S., Jha, P., Xu, Q., Sohn, J. H., Dhaulakhandi, D. B., Kaplan, H. J., and Bora, P. S. (2006) *J. Immunol.* **177,** 1872–1878
10. Bora, N. S., Kaliappan, S., Jha, P., Xu, Q., Sivasankar, B., Harris, C. L., Morgan, B. P., and Bora, P. S. (2007) *J. Immunol.* **178,** 1783–1790
11. Jha, P., Bora, P. S., and Bora, N. S. (2007) *Mol. Immunol.* **44,** 3901–3908
12. Baalasubramanian, S., Harris, C. L., Donev, R. M., Mizuno, M., Omidvar, N., Song, W. C., and Morgan, B. P. (2004) *J. Immunol.* **173,** 3684–3692
13. Harris, C. L., Hanna, S. M., Mizuno, M., Holt, D. S., Marchbank, K. J., and Morgan, B. P. (2003) *Immunology.* **109,** 117–126
14. Fraser, D. A., Harris, C. L., Smith, R. A., and Morgan, B. P. (2002) *Protein Sci.* **11,** 2512–2521
15. Fraser, D. A., Harris, C. L., Williams, A. S., Mizuno, M., Gallagher, S., Smith, R. A., and Morgan, B. P. (2003) *J. Biol. Chem.* **278,** 48921–48927
16. Smith, G. P., and Smith, R. A. (2001) *Mol. Immunol.* **38,** 249–255
17. Sohn, J. H., Kaplan, H. J., Suk, H. J., Bora, P. S., and Bora, N. S. (2000) *Invest. Ophthalmol. Vis. Sci.* **41,** 4195–4202
18. Lyzogubov, V. V., Tytarenko, R. G., Thotakura, S., Viswanathan, T., Bora, N. S., and Bora, P. S. (2009) *Cell Biol. Int.* **33,** 765–771
19. Dot, C., Behar-Cohen, F., BenEzra, D., Doat, M., Jonet, L., May, F., and Jeanny, J. C. (2007) *Exp. Eye Res.* **84,** 1081–1089
20. Schmack, I., Berglin, L., Nie, X., Wen, J., Kang, S. J., Marcus, A. I., Yang, H., Lynn, M. J., Kapp, J. A., and Grossniklaus, H. E. (2009) *Mol. Vis.* **15,** 146–161
21. Dot, C., Parier, V., Behar-Cohen, F., Benezra, D., Jonet, L., Goldenberg, B., Picard, E., Camelo, S., de Kozak, Y., May, F., Soubrane, G., and Jeanny, J. C. (2009) *Mol. Vis.* **15,** 670–684
22. Cole, D. S., and Morgan, B. P. (2003) *Clin. Sci.* **104,** 455–466
23. Halperin, J. A., Taratuska, A., and Nicholson-Weller, A. (1993) *J. Clin. Invest.* **91,** 1974–1978
24. Capey, S., Mosedale, J. G., and van den Berg, C. W. (2007) *Mol. Immunol.* **44,** 608–614
25. Lewis, R. D., Jackson, C. L., Morgan, B. P., and Hughes, T. R. (2010) *Mol. Immunol.* **47,** 1098–1105
26. Acosta, J., Hettinga, J., Flückiger, R., Krumrei, N., Goldfine, A., Angarita, L., and Halperin, J. (2000) *Proc. Natl. Acad. Sci. U.S.A.* **97,** 5450–5455
27. Nauta, A. J., Daha, M. R., Tijsma, O., van de Water, B., Tedesco, F., and Roos, A. (2002) *Eur. J. Immunol.* **32,** 783–792
28. Sato, T., Van Dixhoorn, M. G., Prins, F. A., Mooney, A., Verhagen, N., Muizert, Y., Savill, J., Van Es, L. A., and Daha, M. R. (1999) *J. Am. Soc. Nephrol.* **10,** 1242–1252
29. Hughes, J., Nangaku, M., Alpers, C. E., Shankland, S. J., Couser, W. G., and Johnson, R. J. (2000) *Am. J. Physiol. Renal. Physiol.* **278,** F747–F757